Dynamic Conformations of Flavin Adenine Dinucleotide: Simulated Molecular Dynamics of the Flavin Cofactor Related to the Time-Resolved Fluorescence Characteristics

ARTICLE *in* THE JOURNAL OF PHYSICAL CHEMISTRY B · AUGUST 2002

Impact Factor: 3.3 · DOI: 10.1021/jp020356s · Source: OAI

5 AUTHORS, INCLUDING:

K. Anton Feenstra
VU University Amsterdam
57 PUBLICATIONS **1,131** CITATIONS
SEE PROFILE

Herman J C Berendsen
University of Groningen
296 PUBLICATIONS **58,937** CITATIONS
SEE PROFILE

Antonie Visser
Wageningen University
498 PUBLICATIONS **6,683** CITATIONS
SEE PROFILE

Dynamic Conformations of Flavin Adenine Dinucleotide: Simulated Molecular Dynamics of the Flavin Cofactor Related to the Time-Resolved Fluorescence Characteristics

Petra A. W. van den Berg,[†] K. Anton Feenstra,[‡,§] Alan E. Mark,[‡] Herman J. C. Berendsen,[‡] and Antonie J. W. G. Visser*[,†,||]

MicroSpectroscopy Centre, Laboratory of Biochemistry, Wageningen University, Dreijenlaan 3, 6703 HA Wageningen, The Netherlands, Bioson Research Institute & Laboratory of Biophysical Chemistry, University of Groningen, Nijenborgh 4, 9747 AG Groningen, The Netherlands, and Department of Structural Biology, Institute of Molecular Biological Sciences, Vrije Universiteit, De Boelelaan 1083, 1081 HV Amsterdam, The Netherlands

Received: February 6, 2002; In Final Form: June 7, 2002

Molecular dynamics (MD) simulations and polarized subnanosecond time-resolved flavin fluorescence spectroscopy have been used to study the conformational dynamics of the flavin adenine dinucleotide (FAD) cofactor in aqueous solution. FAD displays a highly heterogeneous fluorescence intensity decay, resulting in lifetime spectra with two major components: a dominant 7-ps contribution that is characteristic of ultrafast fluorescence quenching and a 2.7-ns contribution resulting from moderate quenching. MD simulations were performed in both the ground state and first excited state. The simulations showed transitions from "open" conformations to "closed" conformations in which the flavin and adenine ring systems stack coplanarly. Stacking generally occurred within the lifetime of the flavin excited state (4.7 ns in water), and yielded a simulated fluorescence lifetime on the order of the nanosecond lifetime that was observed experimentally. Hydrogen bonds in the ribityl−pyrophosphate−ribofuranosyl chain connecting both ring systems form highly stable cooperative networks and dominate the conformational transitions of the molecule. Fluorescence quenching in FAD is mainly determined by the coplanar stacking of the flavin and adenine ring systems, most likely through a mechanism of photoinduced electron transfer. Whereas in stacked conformations fluorescence is quenched nearly instantaneously, open fluorescent conformations can stack during the lifetime of the flavin excited state, resulting in immediate fluorescence quenching upon stacking.

Introduction

Flavoproteins are an interesting class of enzymes for which to study the dynamic behavior of biomacromolecules. One reason for this is the large amount of detailed information on both the catalytic mechanism and atomic structure that is available for many members of this large family of redox enzymes. The feature that makes these enzymes particularly suitable for investigating the role of conformational dynamics in catalysis is, however, the flavin cofactor itself; this prosthetic group is not only the redox-active group situated in the heart of the active site but is also a naturally fluorescent group emitting green light. In the past decade, time-resolved fluorescence and fluorescence anisotropy studies have yielded information on the dynamics of the active site of a variety of flavoproteins (for an overview, see refs 1 and 2).

A complicating factor in studying the fluorescence properties of these enzymes is the fact that in most flavoproteins the flavin cofactor is noncovalently bound. It is thus possible to detect fluorescence from the free cofactor as well as from the protein-bound one. In enzymes such as glutathione reductase (GR), lipoamide dehydrogenase, and thioredoxin reductase (TrxR), the dissociation constant for the flavin cofactor is very low (pM−nM range). For these enzymes, careful sample preparation is sufficient to avoid traces of free flavin. However, in other flavoenzymes such as ferredoxin NADPH-reductase (FNR) and *p*-hydroxybenzoate hydroxylase, the flavin is less tightly bound. In these cases, the presence of free flavin has to be taken into account, especially when the fluorescence quantum yield of the free flavin cofactor is high compared to that of the protein-bound cofactor. For this, knowledge of the fluorescence properties of free flavin cofactors under the experimental conditions used is required.

For several decades, the physical properties of the isoalloxazine ring and the two most common flavin cofactors, flavin mononucleotide (FMN) and flavin adenine dinucleotide (FAD, Figure 1), have been the subject of investigation (for reviews on electronic and structural properties of flavins, see refs 3−5). The remarkably low fluorescence of FAD with respect to free riboflavin was first reported by Weber.[6] An intramolecular ground-state complex between the isoalloxazine ring and the adenine moiety was proposed to prevail in aqueous solution, resulting in the formation of a nonfluorescent complex. In steady-state fluorescence experiments, the fluorescence quantum yield of FAD was found to be 9 times lower than that of FMN. By enzymatic digestion of the diphosphate bridge of the FAD molecule, the fluorescence intensity increased to equal that of free FMN. From these experiments, it was proposed that FAD exists in two conformations: a so-called "closed" conformation, in which the isoalloxazine and adenine rings interact through

* Corresponding author. E-mail: Ton.Visser@laser.bc.wau.nl. Tel: 31 317 482862. Fax: 31 317 484801.
[†] Wageningen University.
[‡] University of Groningen.
[§] Current address: Department of Pharmacochemistry, Vrije Universiteit, De Boelelaan 1083, 1081 HV Amsterdam, The Netherlands.
[||] Vrije Universiteit.

10.1021/jp020356s CCC: $22.00
Published on Web 07/27/2002

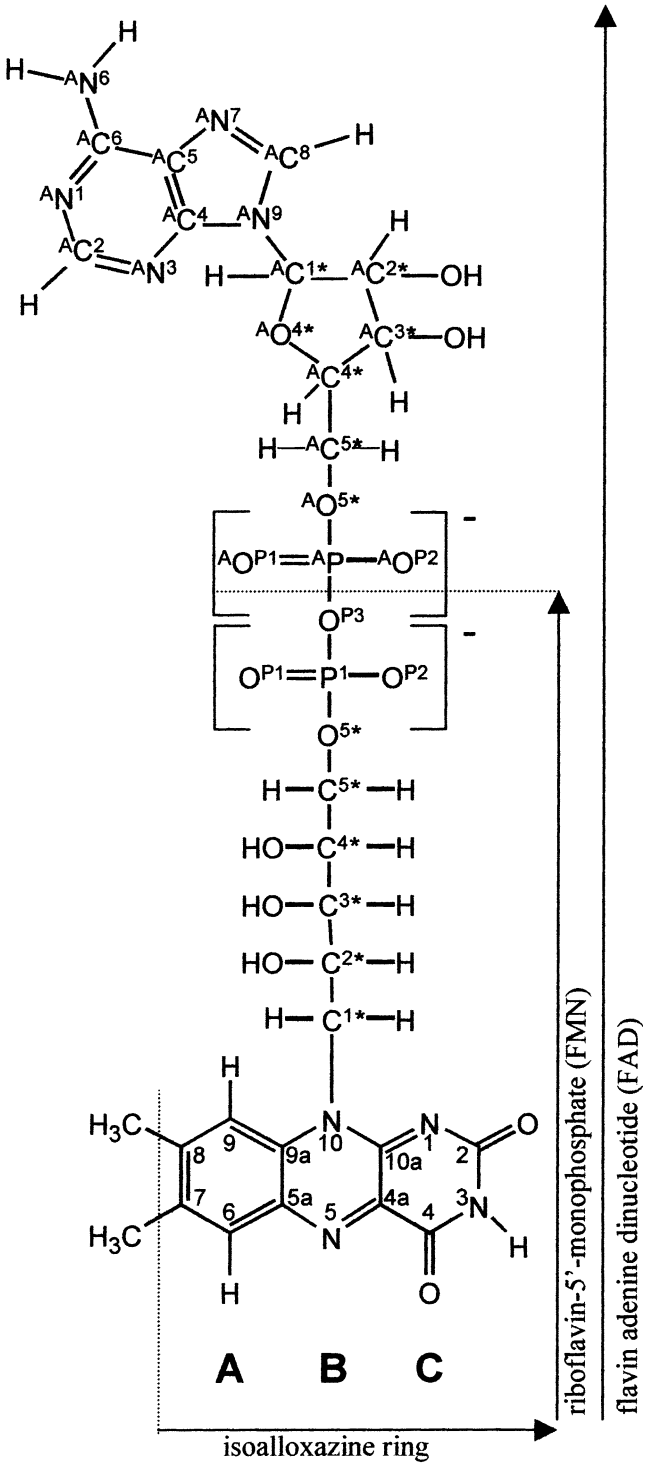

Figure 1. Representation of the structures of FAD and FMN in the oxidized state including atomic labeling. Atom labels for the AMP moiety begin with an A when referred to in the text. In the flavin moiety, the hydrophobic benzene-like ring is ring A, and the pyrimidine-like ring particularly suitable for hydrogen-bonding interactions is ring C.

$\pi-\pi$ interactions in a stacked conformation, resulting in very efficient fluorescence quenching, and an extended, "open" conformation that is responsible for the (remaining) fluorescence of FAD. In solution, the FAD molecule is considered to be predominantly in the stacked conformation. Under the assumption that the equilibrium of stacking and unstacking is the same in the ground state and the first excited state, it can be reasoned that about 80% of the FAD molecules are in the closed conformation and that the lifetime of the intramolecular complex is 27 ns.[7] Dispersion forces are considered to be the principle factor favoring flavin−adenine stacking. Strong acidic conditions, nonpolar solvents, and even polar solvents such as formamide have been reported to prevent complex formation in FAD (ref 8 and references therein).

Although the existence of an open and closed conformation of the FAD molecule is now generally accepted, little is known about the structural details and conformational dynamics in solution. Crystallographic studies on the complex between free riboflavin and the adenosine derivative 5′-bromo-5′-deoxyadenosine revealed an average structure of the $\pi-\pi$ stacked isoalloxazine and adenine ring systems under crystal packing forces.[9,10] In aqueous media, support for a stacked conformation was obtained from ultraviolet resonance Raman spectroscopy, where both chromophores showed Raman hypochromism.[11] From NMR studies, different models were proposed for the interaction between the flavin and adenine moieties, including both intramolecular stacking[12−14] and parallel intramolecular hydrogen bonding between the pyrimidine-like ring of the flavin involving N3 and O4, and the adenine ^{A}NH2 and ^{A}N7.[15] All NMR studies, however, were complicated by the tendency of flavins to form *inter*molecular complexes at millimolar concentrations.

Early time-resolved fluorescence measurements have provided a picture that is consistent with the dynamic model proposed by Weber and co-workers. Decay analysis of FMN revealed a fluorescence lifetime of 4.7 ns, whereas FAD yielded two lifetime components of 2.8 ns (72%) and 0.3 ns (28%), respectively.[16] In the past decade, technical progress has provided a broader time window in which to sample the dynamics of the excited state. Therefore, in this paper, the flavin cofactors are reexamined using subnanosecond resolved time-correlated single-photon counting experiments. Fluorescence lifetime properties, however, relate to the ensemble of molecules and do not yield information on the atomic level. For a proper understanding of the process of stacking and the effect of dynamics on the lifetime of the excited state, a more detailed picture is needed.

In this study, we have investigated the structural dynamics of FAD using a combination of time-resolved fluorescence and MD simulations. Polarized subnanosecond-resolved fluorescence experiments under various temperature and solvent conditions yield experimental data on the dynamic behavior of the flavin cofactor. Nanosecond molecular dynamics simulations in water give insight into the dynamic behavior of the FAD molecule. Changes in the charge distribution were applied to mimic the electronic effect of the transition from the ground state to the excited state following light absorption and to investigate its effect on the dynamics of the molecule. Special attention was given to the interrelation between the MD and fluorescence data in terms of fluorescence quenching and rotational behavior.

Materials and Methods

Time-Resolved Fluorescence and Fluorescence Anisotropy Measurements. Reagents and Sample Preparation. FAD and FMN of the highest purity available were purchased from Sigma. A Biogel P2 column (Biorad) equilibrated with the appropriate measuring buffer was used prior to the fluorescence experiments to remove possible traces of degradation products of FAD. Chromatography experiments with FMN using fluorescence detection showed that FMN did not contain any fluorescent impurities. All measurements were carried out in 50 mM potassium phosphate buffer pH 7.5 except for the control experiments performed in D_2O. Buffers were made from

Nanopure-grade water (Millipore) and were filtered through a 0.22-μm filter (Millipore). The samples had a maximum OD of 0.10 at the wavelength of excitation. Concentrations were calculated from the molar extinction coefficients, $\epsilon_{450\ \mathrm{FAD}} = 11.3\ \mathrm{mM^{-1}\ cm^{-1}}$ and $\epsilon_{445\ \mathrm{FMN}} = 12.5\ \mathrm{mM^{-1}\ cm^{-1}}$.[17] Fluorescent-grade glycerol was purchased from Merck. Sample preparations were performed at 277 K in the dark.

Subnanosecond Polarized Fluorescence. Time-correlated single-photon counting (TCSPC) was used to detect polarized time-resolved fluorescence on a subnanosecond timescale. Details of both the setup and measurement procedures are described elsewhere,[18,19] and only a short outline will be given below. A mode-locked CW Nd/YLF laser was used to pump a cavity-dumped dye laser synchronously. Vertically polarized light of 450 nm (Stilbene 420) or 460 nm (Coumarine) was used to excite the sample with a frequency of 594 kHz and a duration of 4 ps fwhm. The excitation intensity was adjusted to yield a detection frequency of 30 kHz in the parallel component. Parallel and perpendicularly polarized fluorescence was detected through a 557.9-nm interference filter (Schott, Mainz, Germany, half bandwidth of 11.8 nm) in combination with a KV 520 cutoff filter (Schott). FMN data and regular FAD data were collected in a multichannel analyzer with a time window of 1024 channels at typically 15−20 ps/channel. For a better determination of the ultrashort fluorescence lifetime of FAD, a time-window of 8000 channels at typically 3−4 ps/channel was used. The dynamic instrumental response of the setup was obtained at the emission wavelength using erythrosine B in water ($\tau = 80$ ps at 293 K) as a reference compound.[20] This instrumental response function is approximately 40 ps fwhm, which makes the detection of 5−10-ps lifetime components realistic. The temperature of the samples was controlled using a liquid nitrogen flow setup with a temperature controller (model ITC4, Oxford Instruments Inc., Oxford, U.K.).

Analysis of the fluorescence intensity decay $I(t)$ and anisotropy decay $r(t)$ was performed with a model of discrete exponentials using the TRFA data processing package of the Scientific Software Technologies Center of Belarusian State University, Belarus. Global analysis of the total fluorescence decay was performed through linking the fluorescence lifetime constants for multiple data sets, and global analysis of the anisotropy decay was performed through linking the rotational correlation time constants.[21] In addition, data were analyzed through the maximum entropy method (software package from Maximum Entropy Solutions Ltd., Ely, U.K.) in terms of distributions of decay times, for which no a priori knowledge of the system is required.[22] The average fluorescence lifetime $\langle\tau\rangle$ was calculated from the lifetime spectrum $\alpha(\tau)$ according to

$$\langle\tau\rangle = \frac{\sum_{i=1}^{N}\alpha_i\tau_i}{\sum_{i=1}^{N}\alpha_i} \qquad (1)$$

where N is the number of τ_i values of the $\alpha(\tau)$ spectrum. The relative fluorescence quantum yield Q was determined from the TCSPC data as

$$\frac{Q_{\mathrm{FAD}}}{Q_{\mathrm{FMN}}} = \frac{\langle\tau\rangle_{\mathrm{FAD}}}{\langle\tau\rangle_{\mathrm{FMN}}} \qquad (2)$$

A detailed description of the principles of the analysis of the polarized fluorescence data can be found in refs 19, 20, and 23 and references therein.

Molecular Dynamics Simulations. Force Field Description of FAD. The MD simulations were performed with GROMACS 2.0 software.[24] The parameter set for FAD was constructed from parameters taken from the standard building blocks of the GROMOS96 force field for FMN and ATP.[25] Bond lengths and angles and proper and improper dihedral definitions and parameters from the FMN and ATP building blocks were used. For the adenosine moiety and the ribityl chain (from C1* to C5*), partial charges were taken from the GROMOS96 force field. Hydrogen atoms on the adenine and isoalloxazine rings were defined explicitly.[26] Improper dihedrals were added to the bonds on N5 and N10 of flavin ring B (see Figure 1), in accordance with the planar structure observed in crystallographic data and molecular geometry optimizations of flavin in the oxidized state.[27,28] Partial charges on the flavin ring in the ground state and the first excited singlet state were derived from atomic charge densities from ab initio molecular orbital calculations in vacuo on isoalloxazine[29] and semiempirical MINDO-3 calculations on lumiflavin (7,8,10-trimethylisoalloxazine)[30,5] (see Table 1). The charge distribution in the first excited singlet state is similar to that of the first excited triplet state.[30] Partial charges for the pyrophosphate moiety were taken from ab initio molecular orbital calculations on Pi_4 ($H_2P_4O_{13}^{4-}$) as described in ref 31. A full description of the force field parameters, insofar as they are not identical to the GROMOS96 standard building blocks for FMN and ATP, is given in Table 1. A complete description of all force field parameters used is available as Supporting Information.

Starting Structures, Solvation, and Water Equilibration. Starting structures for the unstacked conformation were taken from high-resolution crystal structures of different flavoproteins that contain noncovalently bound FAD. In *E. coli* glutathione reductase (GR)[32] and *E. coli* thioredoxin reductase (TrxR),[33] the flavin cofactor is bound in an almost completely extended conformation. However, in ferredoxin NADPH-oxidoreductase (FNR) from the cyanobacterium *Anabaena*, the flavin cofactor is bound in a distinct bent conformation.[34] The coordinates of the FAD in the above-mentioned crystal structures of GR, TrxR, and FNR were taken to yield three different extended starting structures (FAD-ext1, FAD-ext2, and FADext-3, respectively). For the stacked conformation of FAD, starting structures were generated from unrestrained MD simulations in vacuo of the extended conformation at 300 K using a relative dielectric constant of 10 to mimic the charge-shielding effect of solvent. These in vacuo simulations yielded stacked conformations of the FAD molecule within tens of picoseconds. Two stacked conformations were selected (FAD-sta1, FAD-sta2) in which the adenine moiety stacks on opposite sites of the flavin ring. Care was taken to select frames in which the conformation of the stacked FAD was relatively far away from its energy minimum. All five starting structures were solvated with the extended simple point-charge water model (SPC/E),[35] which provides good correspondence with experimental data for the dynamic behavior of water. A box size of 4.5 nm was chosen to ensure that the minimum distance between the molecule and its periodic images was larger than the cutoff used for the Lennard-Jones interactions (1.0 nm). Depending on the starting structure, the number of water molecules varied between 2407 and 2415. In the next step, energy minimization was carried out using a steepest descents algorithm. Two Na^+ ions were added to the system to compensate for the two negative charges on the phosphate groups by replacing the two water molecules

TABLE 1: Partial Charges on the Isoalloxazine Ring of FAD in the Ground State (S_0) and First Excited Singlet State (S_1) and at Other Positions in FAD[a,b]

(A) partial charges on the isoalloxazine ring in the ground state and first excited singlet state

atom	S_0	S_1	atom	S_0	S_1	atom	S_0	S_1
N1	−0.43	−0.31	C4a	0.06	0.09	C8	0.00	−0.02
C2	0.51	0.48	N5	−0.19	−0.24	C8M	0.00	0.00
O2	−0.45	−0.37	C5a	0.06	0.09	C9	−0.18	−0.17
N3	−0.35	−0.35	C6	−0.12	−0.14	H9	0.19	0.17
H3	0.35	0.35	H6	0.19	0.18	C9a	0.14	0.09
C4	0.43	0.40	C7	0.00	0.00	N10	−0.05	−0.07
O4	−0.43	−0.40	C7M	0.00	0.00	C10a	0.27	0.22

(B) partial charges on the pyrophosphate moiety and surrounding atoms

atom	charge	atom	charge	atom	charge
C5*	0.13	OP2	−1.00	AOP2	−1.00
O5*	−0.52	OP1	−1.00	AO5*	−0.52
P	1.85	AP	1.85	AC5*	0.13
OP3	−0.92	AOP1	−1.00		

(C) partial charges on the adenine ring

atom	charge	atom	charge	atom	charge	atom	charge
AC2	0.22	AHC2	0.14	AC8	0.22	AHC8	0.14

[a] Insofar as they are not identical to the GROMOS96 standard building blocks for FMN and ATP, see reference 25. [b] A full description of the force field parameters is provided as Supporting Information.

with the lowest electrostatic potential. The solvent was pre-equilibrated for 20−30 ps to yield a pressure of 1 bar at 300 K using weak coupling to both an external pressure and temperature bath[36] with harmonic constraints on the atomic coordinates of the FAD molecule. A cutoff of 1.0 nm for Lennard-Jones interactions and short-range electrostatic interactions was applied. Every 20 fs, during neighbor list updates, long-range electrostatics were calculated with a cutoff of 1.6 nm. After equilibration, the length of the box edges was between 4.16 and 4.18 nm.

Simulations of the Molecular Dynamics of FAD in the Ground State and the Excited State. MD simulations were carried out starting from each of the five different starting structures—three in an extended conformation and two in a stacked conformation—with ground-state charges at 300 K. Lennard-Jones and short-range electrostatic interactions were calculated using a cutoff of 1.0 nm. Long-range electrostatic interactions were calculated every 20 fs during the neighbor list update using the particle−particle particle−mesh approach (PPPM).[37,38] A time step of 2 fs was used. After 200 ps, each of the simulations was forked. In one fork, the charges on the isoalloxazine ring were reassigned to correspond to the first excited singlet state (Table 1) to mimic the electronic effects of light absorption. In the other fork, the ground-state charges were maintained. A summary of the simulations performed is presented in Table 2. An eleventh run (FAD-sta3) was generated using the conformation of FAD from the ground-state MD run of starting structure FAD-ext1S0 that had spontaneously stacked in water. In this simulation, the process of light absorption was simulated by again applying excited-state charges using the time frame at 500 ps, where the molecule was in an equilibrated stacked state. To estimate the relative free-energy difference between the open and closed conformations in the ground and excited states, stable trajectories of several nanoseconds in which the molecule remained in the open and closed conformations were required. To obtain more sampling in the open conformation, three additional runs (FAD-ext4S0, FAD-ext4S1, FAD-ext5S1) were performed starting from FAD-ext3S0 (200-ps frame) using different starting velocities. Two additional simulations in the stacked conformation (FAD-sta4S0 and FAD-sta4S1) starting from trajectory FAD-sta3S1 (500 ps frame) were also performed. Individual simulations were run for lengths from 2 to 8 ns, with a total simulation time of approximately 65 ns. An overview of the characteristic parameters of the runs is also presented in Table 2.

TABLE 2: Overview of the Molecular Dynamics Simulations of FAD in Water

run	state	starting structure	simulation time (ns)
FAD-ext1S0	S_0	1gre (glutathione reductase)[a]	0−2.5
FAD-ext1S1	S_1	FAD-ext1S0 at 200 ps[c]	0.2−3.0
FAD-ext2S0	S_0	1tde (thioredoxin reductase)[a]	0−3.7
FAD-ext2S1	S_1	FAD-ext2S0 at 200 ps[c]	0.2−3.7
FAD-ext3S0	S_0	1que (ferredoxin $NADP^+$ reductase)[a]	0−3.7
FAD-ext3S1	S_1	FAD-ext3S0 at 200 ps[c]	0.2−4.2
FAD-ext4S0	S_0	FAD-ext3S0 at 200 ps[d]	0.2−8.2
FAD-ext4S1	S_1	FAD-ext3S0 at 200 ps[d]	0.2−4.2
FAD-ext5S1	S_1	FAD-ext3S0 at 200 ps[d]	0.2−4.2
FAD-sta1S0	S_0	in vacuo stacked FAD-1[b]	0−2.5
FAD-sta1S1	S_1	FAD-sta1S0 at 200 ps[c]	0.2−2.5
FAD-sta2S0	S_0	in vacuo stacked FAD-2[b]	0−2.2
FAD-sta2S1	S_1	FAD-sta2S0 at 200 ps[c]	0.2−2.2
FAD-sta3S1	S_1	FAD-ext1S0 at 500 ps[e]	0.5−2.5
FAD-sta4S0	S_0	FAD-ext1S0 at 200 ps[d]	0.2−8.2
FAD-sta4S1	S_1	FAD-ext1S0 at 200 ps[d]	0.2−8.2

[a] Atomic coordinates for FAD in the open conformation were extracted from the high-resolution crystal structures of three different flavoproteins. The relevant Brookhaven Protein Data Bank entries are given. [b] From in vacuo simulations of FAD, the atomic coordinates of two different stacked conformations were selected and subsequently solvated and treated in the same way as other starting structures. [c] After 200 ps, the electronic effect of light absorption was mimicked by instantaneously adjusting the partial charges appropriate to the first excited singlet state. All other parameters remained unaltered. [d] Simulations were started from the time frame of the indicated trajectory, with starting velocities differing from those of the original run. For FAD-ext4S0 and FAD-ext4S1, identical starting velocities were used. [e] An additional excited-state simulation on FAD that had stacked spontaneously in water was performed using the 500-ps time frame of run FAD-ext1S0. All other parameters remained unaltered.

Analysis of the MD Trajectories. Stacked conformations were defined as having an overlap of the atomic coordinates of the isoalloxazine and adenine rings in the longitudinal and transverse directions, as seen from the plane of the isoalloxazine

SCHEME 1

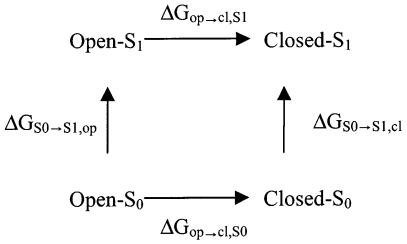

ring (see Figure 1), combined with a maximal distance of 6 Å between the centers of mass of both ring systems perpendicular to the flavin ring. Because the relation between the exact angle between both ring systems and fluorescence quenching is still unclear, no angle criterion was used. Distances between the isoalloxazine and adenine rings were calculated using the center of mass of the ring systems.

To calculate the planarity of the flavin ring, we took the angle between the benzene-like and pyrimidine-like rings of the isoalloxazine ring (rings A and C, respectively, in Figure 1) from the C8−C5a and C10a−N3 vectors. The angle between the isoalloxazine ring and adenine ring was taken from the angle between the planes defined by N5, C9a, and C10a from the flavin and ^{A}N1, ^{A}C2, and ^{A}C8 from the adenine, respectively. The rotational correlation time of the isoalloxazine ring was calculated using the vector C8−N3, which is very close to the direction of the emission dipole moment.[39]

Hydrogen bonds were determined using a simple distance and angle cutoff criterion (donor−acceptor distance ≤0.35 nm and hydrogen donor−acceptor angle ≤60°).[40] To refine the information on hydrogen bonding, the trajectories were analyzed for hydrogen bonds between the different regions of the FAD (flavin ring, ribityl chain, phosphodiester bond, ribofuranosyl, and adenine parts) separately. Cluster analysis of the ribityl−pyrophosphate−ribofuranosyl chain was performed on the atomic positional root-mean-square differences (rmsd) of different backbone conformations from the simulations. A cutoff for the rmsd of 0.1 nm was used to determine neighboring conformations. Cluster analysis was performed according to the following procedure: For each conformation, the number of neighbors is determined. The conformation with the largest number of neighbors is the central structure of the first cluster, and all its neighbors are members of that cluster. These conformations are removed from the pool of all conformations, and the procedure is repeated to generate subsequent clusters until the pool is empty. A complete description of this clustering algorithm is given by Daura et al.[41]

The relative free-energy difference between the open and closed conformations for the ground state and excited state ($\Delta\Delta G^{S0/S1}_{op/cl}$) was calculated using a free-energy perturbation approach[42] in the thermodynamic cycle (Scheme 1). Because the open/closed equilibrium (corresponding to $\Delta G_{op→cl,S0}$ and $\Delta G_{op→cl,S1}$) is computationally inaccessible, the free-energy differences are instead calculated from perturbing the electronic state in the open and closed ensembles, respectively, ($\Delta G_{S0→S1,op}$ and $\Delta G_{S0→S1,cl}$) in a single step:

$$\Delta\Delta G^{S0/S1}_{op/cl} = \Delta G_{op→cl,S0} - \Delta G_{op→cl,S1} = \Delta G_{S0→S1,op} - \Delta G_{S0→S1,cl} \quad (3)$$

$\Delta G_{S0→S1,op}$ and $\Delta G_{S0→S1,cl}$ are calculated from

$$\Delta G_{S0→S1,cl} = G_{S1,cl} - G_{S0,cl} = -RT \ln\langle e^{-\frac{E_{S1}-E_{S0}}{RT}}\rangle_{S0,cl} \quad (4)$$

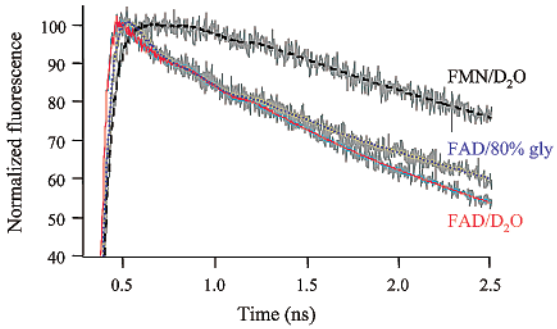

Figure 2. Experimental total fluorescence decays and corresponding theoretical data retrieved from the multiexponential fits of FAD (—) and FMN (− − −) in D_2O and FAD in 50 mM potassium phosphate buffer with 80% glycerol, pH 7.5 (· · ·) at 293 K. Experimental data (grey) and theoretical data (colored) overlay very well. To clearly reveal the differences between the data, only part of the normalized fluorescence intensity decays and only the first part of the 12-ns time window are shown.

where $\langle\cdots\rangle_{S0,cl}$ denotes the average over the closed ensemble in the ground state (S_0) and E_{S0} and E_{S1} represent the energy of the conformations of the ensembles in the ground and excited states, respectively. A total of four simulations were performed, both in open and closed states and in ground and excited states, and all were perturbed to the opposite electronic state in an analogous manner. From these simulations using eq 4, four free-energy differences were calculated ($\Delta G_{S0→S1,cl}$, $\Delta G_{S0→S1,op}$, $\Delta G_{S1→S0,cl}$, and $\Delta G_{S1→S0,op}$). $\Delta G_{S0→S1,cl}$ and $\Delta G_{S1→S0,cl}$ should converge to the same value; likewise, $\Delta G_{S0→S1,op}$ and $\Delta G_{S1→S0,op}$ should converge. From these converged values, $\Delta\Delta G^{S0/S1}_{op/cl}$ can be calculated, and the measure of convergence is a measure of the accuracy.

Results

Fluorescence Dynamics of the Free-Flavin Cofactor. Polarized subnanosecond-resolved TCSPC data of FAD reveal excited-state dynamics over a wider time range than do earlier studies performed at a lower time resolution.[16] Whereas global analysis of the essentially nonquenched fluorescence decay of FMN confirms a predominant lifetime component of 4.7 ns, global analysis of the extraordinarily heterogeneous fluorescence decay of FAD in terms of discrete exponentials yields a lifetime pattern with components covering the dynamic range from picoseconds up to several nanoseconds (Table 3). A predominant lifetime component was found to be on the order of 5−10 ps, which is close to the detection limit of the setup used. This ultrafast fluorescence quenching is reflected in the steep leading edge of the experimental fluorescence decay of the FAD samples (Figure 2) rather than in a separately visible fast decay because of convolution with the pulse (instrumental response of ∼40 ps fwhm) and the slower ingrowth of fluorescence resulting from the nanosecond lifetime component (for similar phenomena in other systems, see refs 2, 18, and 19). At 293 K, the ultrashort component (τ = 7 ps) was found to have a contribution of 83%, whereas a component with a time constant of 2.7 ns had an amplitude of 14%. In addition, a minor percentage of intermediate components (at 293 K: 0.5 ns (1%) and 0.1 ns (2%)) was needed for an optimal description of the excited-state dynamics. Rigorous error analysis at the 67% confidence interval of the global analysis results showed that the time constants of the minor intermediate components are less well defined than those of the major components (Table 3). Analysis in terms of fluorescence lifetime distributions with the MEM method confirmed the general requirement of four lifetime constants

TABLE 3: Fluorescence Lifetime Parameters (τ_i, α_i) and Rotational Correlation Times (ϕ) of FAD and FMN as a Function of Temperature and Solvent Composition[a,b]

			fluorescence lifetime parameters	
sample	T (K)	rotational correlation time ϕ (ns)	lifetime τ_i (ns)	fractional contribution α_i
FAD	277	0.35 (0.32−0.37)	0.008 (0.004−0.008)	0.78 ± 4%
			0.075 (0.072−0.081)	0.11 ± 11%
			0.90 (0.83−1.1)	0.02 ± 15%
			3.6 (3.3−3.8)	0.09 ± 39%
FAD	293	0.20 (0.18−0.23)	0.007 (0.002−0.009)	0.83 ± 3%
			0.10 (0.03−)	0.01 ± 15%
			0.54 (0.37−)	0.02 ± 3%
			2.7 (2.6−3.1)	0.14 ± 7%
FAD	300	0.16 (0.14−0.19)	0.008 (0.003−0.012)	0.72 ± 12%
			0.086 (0.019−)	0.04 ± 63%
			0.55 (0.25−)	0.03 ± 17%
			2.4 (1.9−2.6)	0.20 ± 21%
FAD	313	0.11 (0.10−0.12)	0.010 (0.007−0.011)	0.60 ± 10%
			0.072 (0.052−0.079)	0.12 ± 32%
			1.2 (1.1−1.4)	0.13 ± 36%
			2.2 (1.9−2.8)	0.12 ± 32%
			5.1 (4.6−)	0.02 ± 65%
FAD in 80% glycerol	293	15.1 (14.3−15.8)	0.012 (0.006−)	0.12 ± 140%
			0.13 (0.090−)	0.12 ± 16%
			0.81 (0.69−1.0)	0.22 ± 44%
			4.8 (2.9−5.1)	0.48 ± 17%
			7.1 (5.3−)	0.06 ± 14%
FAD in D_2O	293	0.24 (0.20−0.27)	0.005 (0.002−)	0.81 ± 4%
			0.049 (0.013−)	0.05 ± 6%
			0.44 (0.16−)	0.02 ± 7%
			3.1 (3.0−3.8)	0.11 ± 11%
			6.4 (3.2−)	0.01 ± 9%
FMN in D_2O	293	0.21 (0.18−0.24)	≤0.004[c]	
			0.38 (0.077−)	0.04 ± 17%
			5.3 (5.3−5.4)	0.96 ± 7%
FMN	293	0.18 (0.16−0.20)	1.5 (1.3−1.7)	0.12 ± 2%
			4.7 (4.7−4.8)	0.88 ± 1%

[a] Standard experiments were performed in 50 mM potassium phosphate buffer at pH 7.5. [b] Time constants and fractional contributions (α_i) of the fluorescence lifetime components (τ_i) obtained from global analysis of multiple experiments are presented. The values in parentheses are obtained from a rigorous error analysis at the 67% confidence level, as described in ref 21. For components with low amplitudes, upper confidence limits were not always found. For the fractional contributions α_i, the standard deviation is given. [c] Data suggested the possibility of a third fluorescence lifetime component of a few picoseconds at the border of the detection limit that could not clearly be resolved. This possible component was not taken into account in the fractional contribution calculations.

and yielded identical results. Calculation of the relative fluorescence quantum yield from the amplitudes and time constants of the TCSPC data of FAD and FMN according to eq 2 yielded $Q_{FAD} = 10\%$ of Q_{FMN}, showing rather good agreement with the value of 12% obtained from steady-state fluorescence experiments.[6]

Fluorescence anisotropy decay analysis revealed the overall tumbling motion of the FAD and FMN molecules that are free in solution (Table 3). Increasing the temperature between 277 and 313 K results in a shortening of the rotational correlation time of FAD, which corresponds to the concomitant change in solvent viscosity and kinetic energy (cf. 0.20 ns at 293 K versus 0.16 at 300 K).

In the fluorescence lifetime data, increasing the temperature between 277 and 313 K results in a shortening of the nanosecond decay time. From 293 to 313 K, a clear decrease in the amplitude of the ultrashort lifetime favors the longer lifetime components. This can be explained by a shift in equilibrium toward the open conformation.

A larger shift toward an open, nonquenched conformation is obtained in 80% glycerol (Figure 2 and Table 3), which is consistent with earlier steady-state spectroscopic studies showing that nonpolar solvents prevent stacking interactions (ref 8 and references therein). Measurements of FAD in deuterium oxide revealed only a slight shift of the longest fluorescence lifetime component toward longer time values, leaving the amplitudes virtually unaffected (see Table 3). For FMN, a similar effect on the predominant fluorescence lifetime was obtained. These results show that deuterium oxide slightly influences the intrinsic fluorescence lifetime of the isoalloxazine ring and that significant involvement of hydrogen-bonding interactions in the fluorescence quenching mechanism should not be expected. Fluorescence depolarization analysis of FMN and FAD in deuterium oxide revealed slightly reduced dynamics with respect to water (Table 3).

MD Simulations of the FAD Cofactor and the Process of Light Absorption. The Process of Stacking. To obtain more insight into the relation between the conformational dynamics of the FAD cofactor in solution and the fluorescence characteristics, molecular dynamics simulations were executed. For this study, five different starting structures were used, three of which represent the FAD in an open conformation and two of which represent the flavin and adenine rings in a stacked (or closed) conformation. The electronic effect induced by light

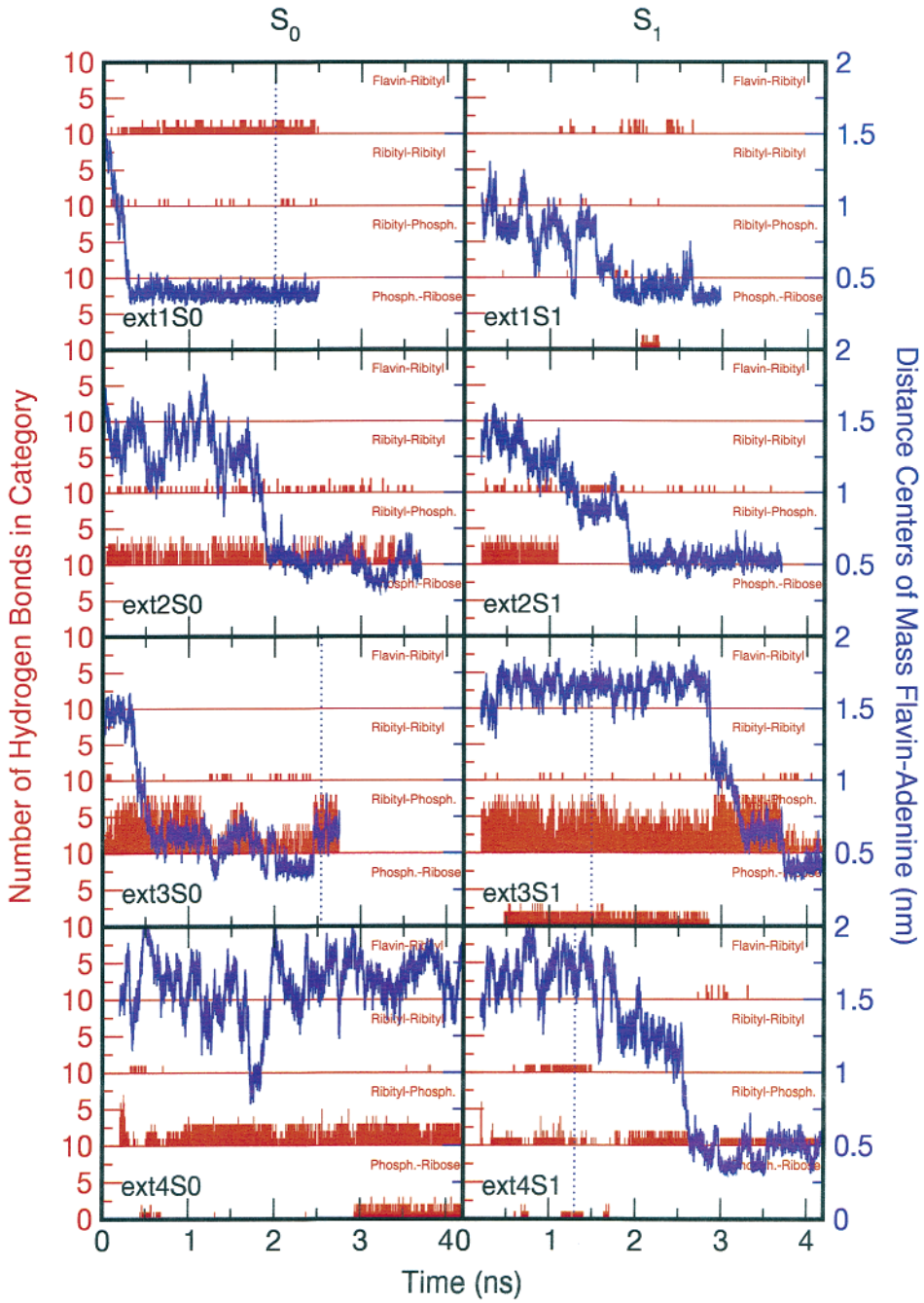

Figure 3. Characteristics of the eight molecular dynamics simulations of FAD starting from the open, extended conformation. The distances between the centers of mass of the flavin and adenine rings are blue. Vertical dotted lines correspond to the snapshots shown in Figure 4. The distance plots provide a good qualitative overview of the changes in molecular conformation during the runs. Conformations with distances of ≤6 Å were regarded as stacked, and those with distances >6 Å, as unstacked (open). Note the regular unstacking in run ext3S0 and the absence of stacking in run ext4S0, which extends up to 8 ns (only the first 4 ns are shown). The number of hydrogen bonds between the flavin ring and the ribityl chain, the ribityl chain and itself, the ribityl chain and the pyrophosphate moiety, and the ribose moiety and the pyrophosphate moiety are shown in red for each of the trajectories (from the upper subpanel downward). Note the presence of hydrogen-bonding networks between the ribose and pyrophoshate moieties and between the ribityl chain and the pyrophosphate moiety in the extended conformation in most of the trajectories. In the stacked conformations, hydrogen bonds between the flavin and ribityl chain can occur (ext1S0, ext1S1, ext4S1).

absorption was simulated by instantaneously adjusting the partial charges on the atoms of the flavin ring. An overview of the simulations performed is given in Table 2.

All MD trajectories, both in the ground state and the excited state, were analyzed for the occurrence of flavin−adenine stacking (for the definition of stacking, see the Materials and Methods section). The distance between the centers of mass of the flavin and adenine ring systems was used to monitor the process of stacking and unstacking and to characterize the FAD conformations (see Figure 3). In one run, the FAD molecule remained in the open conformation throughout the simulation (8 ns). In the other seven runs that were started from open conformations, the isoalloxazine and adenine rings became stacked in the course of the simulation. Whereas in some cases a nearly instantaneous collapse from a completely extended conformation to a highly stable stacked conformation occurred (e.g., complete stacking within a few hundred picoseconds in FAD-ext1S0), other simulations were characterized by the presence of many different intermediates, some of which were relatively long-lived (up to about 1 ns; e.g., FAD-ext2S1, FAD-

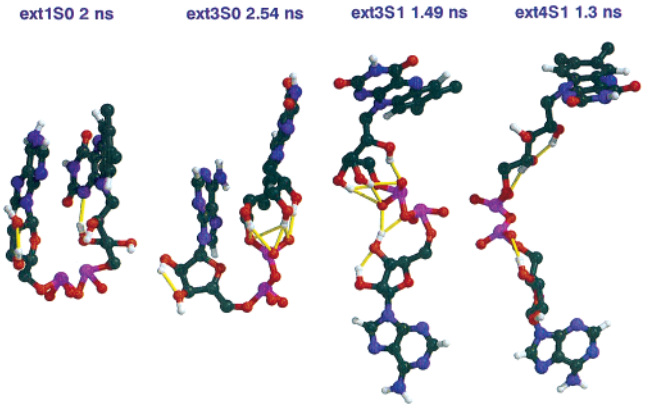

Figure 4. Snapshots of stacked and open conformations observed in the molecular dynamics simulations. Left to right: FAD-ext1S0 at 2.00 ns, FAD-ext3S0 at 2.54 ns, FAD-ext3S1 at 1.49 ns, and FAD-ext4S0 at 1.3 ns. Hydrogen bonds are indicated with yellow lines. Of special interest are the extensive hydrogen-bonding networks involving the phosphate and sugar moieties. Note the strain in the configuration of the phosphate groups.

ext3S1). The simulations revealed that the process of stacking proceeds through the adoption of a more compact but still open conformation in which the ribityl−pyrophosphate−ribofuranosyl chain is bent. The time necessary to reach this conformation appears to be dependent on the presence of particular intramolecular hydrogen-bonding networks. Subsequently, the isoalloxazine and adenine rings come into contact.

The first intramolecular interactions observed between "non-neighboring" parts of the molecule involved, in most cases, the hydrophilic ring of the flavin (particularly O2 and N3, see Figure 1) and the six-membered ring of the adenine. This interaction is sometimes preceded by a contact between the flavin and the (hydroxyl groups of the) sugar. An alternative pathway for stacking involves the disruption of a hydrogen-bonding network between the AMP−phosphate and the sugar. The adenine subsequently moves close to the flavin via the ribityl chain (FAD-ext3S1). After the disruption of a second set of hydrogen bonds (between the ribityl chain and the FMN−phosphate), the six-membered ring of the adenine and the hydrophobic ring of the flavin (ring A in Figure 1) stack. It should be mentioned that different stacking routes result in different closed conformations (see the next section).

Once the flavin and adenine moieties were in a stacked conformation with considerable overlap of the ring systems, unstacking of the flavin and adenine rings occurred only occasionally and was brief (generally a few to 50 ps at most). Hardly any complete unstacking of the flavin and adenine rings was observed in molecules with full stacking between the rings (FAD-ext1, FAD-sta1, FAD-sta2, FAD-sta3; for the runs starting from stacked conformations, data are not shown), irrespective of the electronic state of the flavin. The less overlap between the ring systems in the stacked state, the easier was the unstacking. In the run FAD-ext3S0, a closed conformation with proper stacking was hampered (see Figure 4). Here, unstacking of the rings lasting up to several hundreds of picoseconds was more common. However, the FAD remained in a compact state with the adenosine and ribityl moieties in contact. In none of the simulations was unfolding of the molecule to a fully extended conformation observed.

To determine whether the process of light absorption influences the equilibrium between the open and closed conformations of FAD, free-energy calculations were performed to determine $\Delta\Delta G$ of the stacking transition in the ground state

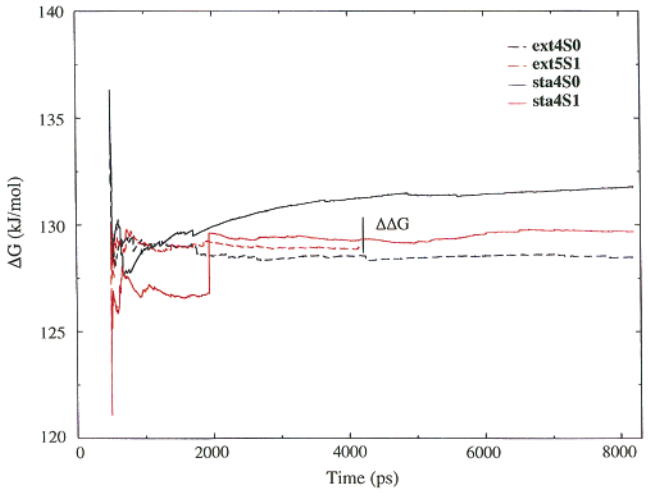

Figure 5. Cumulative average of the relative free energy of stacking in the ground state and the excited state. For the stacked conformations, two additional runs starting from the conformation stacked in water (starting with the frame at 500 ps from trajectory FAD-ext3S0) were performed to yield 8 ns of data for both the ground state and the excited state. For the open conformations, the 8-ns trajectory of FAD-ext4S0 and an additional run in the excited state yielding 4.2 ns of open conformations were used. Relative free energies for the ground state and first excited state were calculated using both charge distributions for the same trajectory. For the stacking transition, no significant free-energy difference between the ground state and the excited state was observed.

and in the excited state using the thermodynamic cycle as depicted in Scheme 1 and eq 3. Free-energy calculations yielded similar time-averaged energy differences between the stacked and unstacked conformation for the ground state and for the excited state, in principle suggesting that in fluorescence the process of light absorption does not influence the conformational equilibrium (Figure 5). From Figure 5, it can be seen that the convergence between forward and backward perturbations is of the same size as the resulting $\Delta\Delta G$, indicating that, because of the long-lived conformational states, statistics are the limiting factor in obtaining an accurate estimate for $\Delta\Delta G$.

The Conformational Landscape: Clusters of Conformations. The range of conformations observed for the FAD molecule can be best described by the relative positions and orientations of the flavin and adenine rings and the conformation of the connecting ribityl−pyrophosphate−ribofuranosyl backbone. This information is summarized in Table 4. Note that the stacked starting structures FAD-sta1 and FAD-sta2 were created in vacuo whereas the other stacked conformations were produced in solution. It appears that in solution the adenine ring can stack on either side of the flavin and there is no preferred orientation of the ribityl−pyrophosphate−ribofuranosyl backbone. In general, the isoalloxazine and adenine rings stack coplanarly. In water, FAD tends to adopt a fully parallel stacked conformation similar to those created in vacuo (average angle between the flavin and adenine planes = 12.5°). In several simulations, (intermediate) conformations were found in which the flavin and adenine rings were slightly tilted (about 30°, see Table 4) but still had substantial contact. Occasionally, water molecules intercalated on one of the edges between the rings, and a hydrogen-bonded water bridge formed between the rings, resulting in decreased coplanarity. Stacking also influenced the planarity of the flavin ring system. Whereas in the open conformations an average angle of 15° was found between rings A and C of the isoalloxazine (Figure 1), this angle was slightly, but systematically, smaller in the stacked conformations (13°,

TABLE 4: Overview of Parameters Characterizing the Dynamic Behavior and the Stacked Conformations in the Molecular Dynamics Simulations[a]

		stacked conformations[c]				average θ flavin[d]		rotational correlation time (ps)	
run	stacking time (ns)[b]	position	chain	plane	θ fla-ade	open	stacked	open	stacked
FAD-ext1S0	0.26	C	R	Si	11.0 ± 6.5	16.0 ± 7.9	11.6 ± 6.4	−	131.1
FAD-ext1S1	1.24	C/BC	R	Si	13.2 ± 8.2	18.2 ± 8.9	14.0 ± 8.4	116.9	146.6
FAD-ext2S0	1.86	C	R	Si	31.3 ± 18.3	15.5 ± 8.0	13.7 ± 7.5	149.5	194.6
FAD-ext2S1	1.87	C	R	Si	34.6 ± 9.4	13.8 ± 7.7	13.9 ± 7.3	131.1	234.7
FAD-ext3S0	0.62	A	S	Re	26.0 ± 14.8	13.9 ± 8.0	13.6 ± 7.5	115.5	144.1
FAD-ext3S1	3.28	B	S	Re	12.3 ± 8.5[e] 35.3 ± 13.7	14.4 ± 8.0	13.6 ± 7.5	118.6	146.2
FAD-ext4S0	>8.2	−	−	−	−	14.9 ± 8.3	−	121.9	−
FAD-ext4S1	2.63	BC	S	Si	30.3 ± 23.1	14.3 ± 8.2	17.3 ± 8.4	173.3	204.0
FAD-sta1S0	−	BC	S	Si	13.0 ± 8.2[e] 37.1 ± 11.4	−	12.9 ± 7.1	−	176.7
FAD-sta1S1	−	BC	S	Si	13.1 ± 7.5	−	12.3 ± 6.2	−	132.8
FAD-sta2S0	−	BC	S	Re	12.2 ± 7.2	−	10.9 ± 6.0	−	127.4
FAD-sta2S1	−	BC	S	Re	11.8 ± 7.0	−	11.6 ± 6.5	−	143.9
FAD-sta3S1	−	C	R	Si	13.0 ± 9.1	−	12.0 ± 6.7	−	116.3

[a] Parameters that could not be retrieved because of the absence (or limited existence) of a particular conformation or transition are indicated by the symbol −. [b] Only the time interval for the first transition from an open to a stacked conformation is given. Unstacking (rapidly) followed by restacking was observed regularly. FAD-ext3S0 and FAD-ext1S1 (single event) had long periods of unstacking (up to 250 ps). For further details, see the Results section and the Figures 3 and 4. [c] The following characteristics of the stacked conformations are presented: (1) Average relative positions of the adenine and isoalloxazine rings. The ring(s) that is (are) closest to the center of mass of the adenine is (are) given. The labels of the rings (A = hydrophobic ring, B = middle ring, C = hydrophilic ring) are clarified in Figure 1. (2) Direction in which the ribityl−pyrophosphate−ribofuranosyl chain is twisted (going from the flavin to the adenine) with R = clockwise and S = counterclockwise. (3) Side of the isoalloxazine plane on which the adenine stacks. Si = on the front, and Re = on the back of the isoalloxazine ring, as depicted in Figure 1. (4) Average angle θ between the adenine and flavin rings in the stacked conformation. [d] Average angle θ between rings A and C of the isoalloxazine ring in the open and stacked conformations. [e] Clear transitions to conformations in which the flavin and adenine rings are slightly tilted (angle of about 35°) were found for FAD-sta1S0 (1.2−2.4 ns) and FAD-ext3S1 (3.3−3.7 ns).

see Table 4). The largest deviations from planarity were found during conformational transitions involving intramolecular interactions with the isoalloxazine ring. After stacking, the flavin and adenine had some lateral freedom but were restricted by the conformation of the connecting chain. In general, this mobility decreased with the increasing overlap of the rings. The average position of the stacked ring systems was not influenced by the changed charge distribution from the ground state to the excited state. In many of the stacked conformations, a high strain occurred on one or both of the phosphate groups, resulting in a significant deviation from the tetrahedral configuration. This deviation may be due to an overestimate of charge interactions in the force field of the phosphodiester bridge because these charge interactions are abundant in the stacked conformation.

The conformations of the ribityl−pyrophosphate−ribofuranosyl backbone connecting the flavin and adenine moieties were analyzed through the rmsd of the atomic positions and were grouped in clusters of highly similar conformations. From the cluster analysis, it can be concluded that in runs from different starting structures different conformations of the backbone chain were sampled and that only a few transitions from one cluster to another occurred. Specific dihedral configurations of the backbone chain stabilized by hydrogen-bond networks appear to have very long lifetimes, thereby restricting the rings to certain conformations. Conversely, in the stacked situation, the strong interactions between the rings may restrict rearrangements of the backbone chain. Surprisingly, the starting structures stacked in vacuo have backbone conformations differing distinctly from the structures resulting from stacking in water. This is also reflected in the relative positions of the stacked rings, as shown in Table 4.

Conformational Fluctuations and Mobility: Hydrogen Bonding, Solvent Interactions, and Rotational Correlation. An important conclusion from the MD simulations is that in solution the backbone of the FAD molecule behaves much more rigidly than we had expected. To gain insight into the effect of hydrogen bonds between the different building blocks of FAD, the trajectories were analyzed in terms of the number of hydrogen bonds between two separate regions of the molecule (flavin ring, ribityl chain, pyrophosphate, ribofuranosyl, and adenine ring). The high density of hydrogen-bonding donors and acceptors in the chain provides an excellent framework for intramolecular hydrogen bonding. Intramolecular hydrogen-bond networks between the sugar and the phosphodiester bond appear to have a prominent effect on the lifetime of the open conformation (see Figure 3). Hydrogen bonding between the ribityl chain and the phosphodiester bond contributes to this lifetime as well. For this network, the number of hydrogen bonds may even temporarily increase just before stacking because upon bending of the chain the distant phosphate comes within hydrogen-bonding distance of the ribityl chain as well (e.g., ext3S1). Both the formation of hydrogen bonds and the concomitant breaking of the hydrogen bonds appeared to be highly cooperative. The breaking up of a cooperative network involves a free-energy barrier that can "lock" the molecule into a particular open conformation for long periods of time (up to hundreds of picoseconds). The interplay between the energetically favorable stacking of the ring systems on one hand and the cooperative hydrogen bond formation between the ribityl chain and the FMN−phosphate on the other hand resulted in frequent stacking, unstacking, and restacking in the same conformation (FAD-ext3S0).

In some stacked conformations, especially in FAD-ext1, a hydrogen bond was formed between the hydroxyl group attached to C4* or C3* of the ribityl chain and N1 of the flavin. In the literature, the interaction between a hydroxyl group of the ribityl chain and N1 of the flavin was proposed to be involved in the intramolecular photoreduction of the flavin, resulting in subsequent photodegradation.[43] As a candidate for this, the hydroxyl group of C2* of the ribityl chain was proposed. This hydrogen bond was found in the MD simulations as well, but only on rare occasions.

In all MD runs, one Na^+ ion was either initially positioned 2 Å from the ester oxygen of the phosphodiester bond or it migrated to this position during the run (between 0.1 and 2 ns). Sometimes, the second Na^+ ion moved toward this position as well. No interactions between Na^+ ions and the flavin ring were found.

The rotational mobility of the FAD molecules was analyzed through a second-order Legendre polynomial of the autocorrelation function pertaining to the rotational orientation of the flavin ring. For this analysis, the N3−C8 axis, whose direction is very close to that of the emission dipole moment[39] was used. The rotational correlation time of the flavin was 149 ± 33 ps. A small difference was found between the rotational correlation time of the flavin in the stacked and the unstacked parts of the simulations. Analysis of the trajectories in which only the stacked conformations were taken into account resulted in a rotational correlation time of 162 ± 35 ps, whereas for the unstacked conformations, a time constant of 132 ± 22 ps was found. In every run in which the molecule was in both an unstacked and a stacked conformation for a considerable period of time, the rotational correlation time for the unstacked situation was significantly smaller than that for the stacked (Table 4). This may be explained by additional mobility of the isoalloxazine ring in the plane perpendicular to the ribityl−pyrophosphate−ribofuranosyl backbone. As in time-resolved fluorescence experiments the signal of the anisotropy decay is fully carried by the nanosecond lifetime component stemming from the open conformations, comparisons between the rotational correlation times obtained from experiment and simulations should regard the unstacked conformations. Given the limited statistics of the unstacked conformations, these values are in good agreement (from simulations, 132 ± 22 ps; from experiment, 160 ps at 300 K; Tables 3 and 4).

Discussion

In this study, we have demonstrated the combined use of molecular dynamics simulations and (sub)nanosecond-resolved fluorescence spectroscopy to obtain more detailed insight into the dynamic structure of complex fluorophores such as the flavin adenine dinucleotide cofactor. Polarized fluorescence experiments with high time resolution yield a broad picture of the dynamic landscape for the ensemble of molecules in solution, whereas MD simulations provide a detailed view of the underlying molecular structures and possible transition pathways. The limitation, however, is whether it is possible to run simulations that are long enough to sample the conformational space sufficiently.

The molecular dynamics simulations confirm that the FAD molecule in aqueous solution is predominantly in a compact conformation in which the flavin and adenine moieties are stacked. Although unstacking of the flavin and adenine ring systems occurs, the molecule is mainly in a conformation in which the flavin and adenine rings can have (large) $\pi-\pi$ overlap, occasionally alternated by conformations in which the ring systems interact via direct or water-mediated hydrogen bonds.

These simulations suggest that several potential quenching mechanisms for ultrarapid fluorescence quenching in FAD are unlikely. Although sampling of the open/closed equilibrium was far from complete in our simulations, extensive sampling of the closed state yielded reasonable statistics on the propensity of hydrogen bond formation in the closed state. In the MD simulations, interactions between the flavin N5 and the amino group of the adenine ring were observed only rarely and were mostly bridged through a water molecule. A perpendicular orientation of the flavin and the adenine in which the lone electron pair of N5 could interact with the π system of the adenine was not found at all. It is therefore improbable that a quenching mechanism based upon these interactions gives rise to the predominant picosecond fluorescence lifetime component that was observed. Likewise, a quenching mechanism involving hydrogen bonding between the adenine and the 2-keto function of the flavin as proposed by Tsibris et al.,[44] is also unlikely on the basis of the virtual absence of such interactions in the simulations. Fluorescence experiments in deuterium oxide did not give any evidence for the involvement of hydrogen bonds in fluorescence quenching either. In addition, the absence of substantial hydrogen bonding between the flavin and adenine moieties renders a significant population of molecules with parallel intramolecular hydrogen bonding between the flavin and adenine, as proposed by Raszka and Kaplan[15] for the unstacked state, highly unlikely.

The stacked conformation of the flavin and adenine rings observed in the MD simulations, however, can well explain the ultrarapid fluorescence quenching in FAD. The MD simulations reveal a large overlap of the coplanar flavin and adenine ring systems indicating large $\pi-\pi$ overlap. The interactions between the adenine and isoalloxazine rings may yield additional deexcitation routes through internal conversion. Most likely, however, the mechanism of flavin fluorescence quenching involves a photoinduced charge-transfer interaction between the adenine (donor) and flavin (acceptor). Photoinduced electron (or hydrogen) transfer from electron-rich donors to the isoalloxazine is a well-known property of flavins.[18,45−47] In flavoproteins that contain a tyrosine or tryptophan residue adjacent to the flavin, photoinduced electron transfer to the flavin has been shown to result in highly efficient flavin fluorescence quenching with time constants in the picosecond and subpicosecond ranges.[18,19,47−49] Although classical charge-transfer interactions between flavin and purines have been reported not to contribute significantly in the ground state, photoinduced electron transfer should be considered for ultrafast excited-state quenching in the complex. For photoinduced electron transfer, the relation between the free energy of the reaction, the reorganization energy, and the distance between the donor and acceptor is expressed in the Rehm−Weller equation.[50,51] On the basis of the redox potentials for adenine reported by Seidel et al.[52] (about 1.5 V at pH 7.5) and FMN (−0.24 V)[53], photoinduced electron transfer is likely to occur at the wavelength of excitation (energy for the $S_0 \rightarrow S_1$ transition ($\pi-\pi^*$ character) at 450 nm is 2.76 eV). In general, typical rate constants for electron transfer derived from a variety of biological and (semi)-synthetical systems are on the order of 1 to 0.1 ps^{-1} for donor−acceptor distances of 5 Å, whereas distances of 10 Å generally result in rates between 10 and 1 ns^{-1}.[54] The picosecond fluorescence quenching observed for FAD corresponds to a rate constant of ∼0.15 ps^{-1}, which lies in the expected time range for electron transfer. Because the time constant is close to the detection limit of the TCSPC setup that was used, the rate constant for quenching might be somewhat underestimated. Recently, femtosecond fluorescence quenching was observed in the flavoproteins riboflavin-binding protein[47,49] and the D-amino acid oxidase/benzoate complex[49] that contain a (coplanarly) stacked complex between the isoalloxazine ring and an aromatic ring (trp and tyr, and benzoate, respectively). Such ultrafast processes would fall beyond the detection limit of our experimental setup. The oxidation potentials of tryptophan and tyrosine, however, are somewhat lower than that of adenine,

thus accelerating an electron transfer reaction. Recently reported transient-absorption spectra of FAD revealed a time constant for excited-state quenching of about 4 ps,[55] which is in close agreement with the results presented here. Although the study on the transient absorption of FMN and FAD in water and formamide definitely confirmed the rapid excited-state quenching of flavin−purine complexes in aqueous solution, the molecular mechanism of quenching was not discussed.

Besides the picosecond fluorescence lifetime component discussed above, the fluorescence lifetime patterns of FAD contained a nanosecond component and minor but definite contributions of intermediate time constants (100 ps−1 ns). In an extreme model considering each component of the lifetime spectrum as a separate conformational state with a conformational lifetime longer than the fluorescence lifetime of that particular state (conformational substates model), these could be interpreted as separate conformations of the FAD molecule with a (very) small but significant population. In the simulations, however, we observed the FAD molecule to experience conformational transitions during the lifetime of the excited state on time scales ranging from several tens of picoseconds to nanoseconds. In such a dynamic environment, the amplitude of a particular fluorescence lifetime that is observed reflects the total number of dynamic processes for all conformations encountered that lead to fluorescence quenching with that particular time constant. In this situation, a direct link between the amplitudes of fluorescence lifetime components and the population of certain conformational states cannot be made.

On the basis of the fluorescence characteristics of FMN together with the MD simulations, however, we believe that for FAD in the stacked conformation only, the flavin fluorescence will be quenched immediately. When the picosecond fluorescence lifetime constants of FAD represents the closed conformation, and the other lifetimes the (various) open conformations of the molecule, one can obtain estimates of the populations. Under the assumptions that only the observed ultrafast component reflects the stacked conformation and that the equilibrium constant for the excited state is identical to that for the ground state (which seems reasonable from the calculations of the free-energy differences for the stacking equilibrium in the ground state and the excited state), the population of FAD molecules in the open conformations, as calculated from the weight of the amplitudes from the TCSPC data, is about 17% at 293 K.

The open, unstacked conformations of FAD are responsible for the significant 2.7-ns fluorescence lifetime component. The MD simulations have shown that the FAD molecule can exist in an extended conformation for considerable periods of time, which are longer than the intrinsic fluorescence lifetime of the flavin. However, if a considerable number of FAD molecules remain in an extended open conformation with no intramolecular interactions between the flavin and adenosine moieties during the lifetime of the excited state, a nanosecond fluorescence lifetime constant identical to that of FMN (4.7 ns) would be expected. An explanation for the 2.7-ns lifetime component of FAD that cannot be fully excluded is the existence of a particular compact conformation with a long conformational lifetime (compared to the lifetime of the excited state) in which the flavin does not stack but interacts with other parts of the molecule, resulting in less efficient flavin fluorescence quenching. It is interesting that in the FAD-ext3S0 run, the long-lived conformation in which the flavin and adenine moieties are close to each other but do not stack (Figure 4) resembles the X-ray structure of the FAD cofactor bound to DNA photolyase,[56] the only flavoprotein known thus far in which the cofactor is bound in a nonextended conformation. This particular conformation, however, occurred persistently in one run only, which is not sufficient to explain the magnitude of the 2.7-ns fluorescence component.

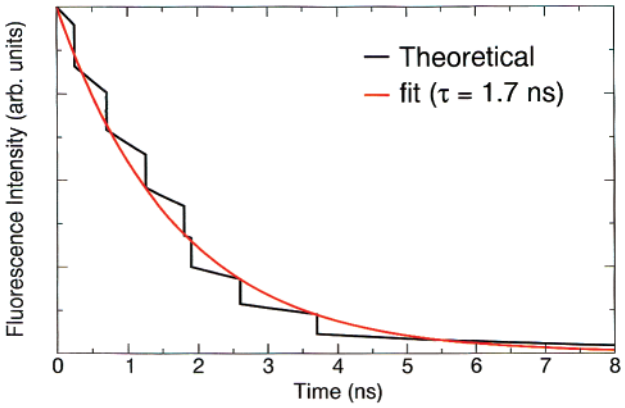

Figure 6. Hypothetical fluorescence decay curve calculated from the molecular dynamics simulations under the assumptions that (1) the limited number of FAD starting structures in the extended conformation adequately represents the conformational ensemble of open FAD molecules in solution; (2) the dynamics of the molecule are not significantly influenced by light excitation; and (3) any stacked conformation will instantaneously quench. Both ground- and excited-state traces were included to obtain better statistics because no significant difference between the ground- and excited-state dynamics was detected (see also free-energy calculations, assumption 2). The intrinsic fluorescence decay of the flavin was taken into account by multiplying the simulated curve by the fluorescence decay curve corresponding to the fluorescence lifetime of nonquenched flavin in water, such as in FMN (τ = 4.7 ns). From curve fitting with a monoexponential decay model, a theoretical fluorescence lifetime of 1.7 ns was obtained.

Therefore, a more likely hypothesis is that the nanosecond fluorescence lifetime component of FAD corresponds to the conformational lifetime of the open conformation. Support for this is found in the MD simulations, where except for one run all simulations starting from an extended conformation of the molecule stacked within 5 ns. From these simulations, a hypothetical fluorescence decay curve can be constructed (Figure 6) under the assumptions that the limited ensemble of FAD starting structures in the extended conformation adequately represents the conformational ensemble of open FAD molecules in solution, that the dynamics of the FAD are not significantly influenced by light excitation, and that as soon as a FAD molecule stacks, quenching occurs. The theoretical fluorescence lifetime retrieved from this hypothetical curve is 1.7 ns, which is not far from the nanosecond lifetime observed with time-resolved fluorescence (2.4 ns at 300 K). The time-resolved fluorescence data and molecular dynamics simulations support the idea that the majority of FAD molecules are in a closed conformation in which the adenine and flavin rings are stacked and that a small percentage of FAD molecules can remain in the open conformation for nanoseconds of time.

Acknowledgment. We thank B. Hess for adjustments of the software package, Dr. D. van der Spoel for assistance in early MD pilot experiments, A. van Hoek for help with the fluorescence experiments, and Dr. W. J. H. van Berkel for valuable discussions and suggestions. This work was supported by the Netherlands Foundation for Chemical Research (SON) with financial aid from the Netherlands Organization for Scientific Research (NWO).

Supporting Information Available: Complete description of all force field parameters used. This material is available free of charge via the Internet at http://pubs.acs.org.

References and Notes

(1) van den Berg, P. A. W.; Visser, A. J. W. G. In *New Trends in Fluorescence Spectroscopy: Applications to Chemical and Life Sciences*; Valeur, B., Brochon, J.-C., Eds.; Springer: Berlin, 2001; p 457.

(2) van den Berg, P. A. W.; Mulrooney, S. B.; Gobets, B.; van Stokkum, I. H. M.; van Hoek, A.; Williams, C. H., Jr.; Visser, A. J. W. G. *Protein Sci.* **2001**, *10*, 2037.

(3) Song, P. S. In *Quantum Aspects of Heterocyclic Compounds in Chemistry and Biochemistry*; Bergmann, E. D., Pullman, B., Eds.; Israel Academy of Sciences and Humanities: Jerusalem, 1970; p 358.

(4) Leijonmarck, M. *Chem. Commun.* **1977**, *8*, 1.

(5) Hall, L. H.; Orchard, B. J.; Tripathy, S. K. *Int. J. Quantum Chem.* **1987**, *31*, 217.

(6) Weber, G. *Biochem. J.* **1950**, *47*, 114.

(7) Spencer, R. D.; Weber, G. In *Structure and Function of Oxidation Reduction Enzymes*; Åkeson, Å., Ehrenberg, A., Eds.; Pergamon Press: Oxford, 1972; p 393.

(8) Penzer, G. R.; Radda, G. K. *Q. Rev., Chem. Soc.* **1967**, *21*, 43.

(9) Voet, D.; Rich, A. In *Flavins and Flavoproteins*; Kamin, H., Ed.; University Park Press: Baltimore, MD, 1971; p 23.

(10) Voet, D.; Rich. A. *Proc. Natl. Acad. Sci. U.S.A.* **1971**, *68*, 1151.

(11) Copeland, R. A.; Spiro, T. G. *J. Phys. Chem.* **1986**, *90*, 6648.

(12) Sarma, R. H.; Dannies, P.; Kaplan, N. O. *Biochemistry* **1968**, *7*, 4359.

(13) Kotowycz, G.; Teng, N.; Klein, M. P.; Calvin, M. *J. Biol. Chem.* **1969**, *244*, 5656.

(14) Kainosho, M.; Kyogoku, Y. *Biochemistry* **1972**, *11*, 741.

(15) Raszka, M.; Kaplan, N. O. *Proc. Natl. Acad. Sci. U.S.A.* **1974**, *71*, 4546.

(16) Visser, A. J. W. G. *Photochem. Photobiol.* **1984**, *40*, 703.

(17) Whitby, L. G. *Biochem. J.* **1953**, *54*, 437.

(18) van den Berg, P. A. W.; van Hoek, A.; Walentas, C. D.; Perham, R. N.; Visser, A. J. W. G. *Biophys. J.* **1998**, *74*, 2046.

(19) Visser, A. J. W. G.; van den Berg, P. A. W.; Visser, N. V.; van Hoek, A.; van den Burg, H. A.; Parsonage, D.; Claiborne, A. *J. Phys. Chem.* **1998**, *102*, 10431.

(20) Bastiaens, P. I. H.; van Hoek, A.; Wolkers, W. F.; Brochon, J. C.; Visser, A. J. W. G. *Biochemistry* **1992,** *31*, 7050.

(21) Beechem, J. M. *Methods Enzymol.* **1992**, *210*, 37.

(22) Brochon, J. C. *Methods Enzymol.* **1994**, *240*, 262.

(23) Digris, A. V.; Skakoun, V. V.; Novikov, E. G.; van Hoek, A.; Claiborne, A.; Visser, A. J. W. G. *Eur. Biophys. J.* **1999**, *28*, 526.

(24) Berendsen, H. J. C.; van der Spoel, D.; van Drunen, R. *Comput. Phys. Commun.* **1995**, *91*, 43.

(25) van Gunsteren, W. F.; Billeter, S. R.; Eising, A. A.; Hünenberger, P. H.; Krüger, P.; Mark, A. E.; Scott, W. R. P.; Tironi, I. G. *Biomolecular Simulation: The GROMOS96 Manual and User Guide*; BIOMOS b.v.: Zürich, Groningen, 1996.

(26) van der Spoel, D.; van Buuren, A. R.; Tieleman, D. P.; Berendsen, H. J. C. *J. Biomol. NMR* **1996**, *8*, 229.

(27) Zheng, Y. J.; Ornstein, R. L. *J. Am. Chem. Soc.* **1996**, *118*, 9402.

(28) Meyer, M.; Hartwig, H.; Schomburg, D. *J. Mol. Struct.* **1996**, *364*, 139.

(29) Platenkamp, R. J.; Palmer, M. H.; Visser, A. J. W. G. *J. Mol. Struct.* **1980**, *67*, 45.

(30) Teitell, M. F.; Suck, S. H.; Fox, J. L. *Theor. Chim. Acta* **1981**, *60*, 127.

(31) van der Spoel, D.; Feenstra, K. A.; Hemminga, M. A.; Berendsen, H. J. C. *Biophys. J.* **1996**, *71*, 2920.

(32) Mittl, P. R. E.; Schulz, G. E. *Protein Sci.* **1994**, *3*, 799.

(33) Waksman, G.; Krishna, T. S. R.; Williams, C. H., Jr.; Kuriyan, J. *J. Mol. Biol.* **1994**, *236*, 800.

(34) Serre, L.; Vellieux, F. M. D.; Medina, M.; Gomez-Moreno, C.; Fontecilla-Camps, J. C.; Frey, M. *J. Mol. Biol.* **1996**, *263*, 20.

(35) Berendsen, H. J. C.; Grigera, J. R.; Straatsma, T. P. *J. Phys. Chem.* **1987**, *91*, 6269.

(36) Berendsen, H. J. C.; Postma, J. P. M.; van Gunsteren, W. F.; DiNola, A.; Haak, J. R. *J. Chem. Phys.* **1984**, *81*, 3684.

(37) Hockney, R. W.; Eastwood, J. W. *Computer Simulation Using Particles*; IOP Publishing Ltd.: Bristol, U.K., 1988.

(38) Luty, B. A.; van Gunsteren, W. F. *J. Phys. Chem.* **1996**, *100*, 2581.

(39) Bastiaens, P. I. H.; van Hoek, A.; Benen, J. A. E.; Brochon, J. C.; Visser, A. J. W. G. *Biophys. J.* **1992**, *63*, 839.

(40) Kabsch, W.; Sander, C. *Biophys. J.* **1983**, *22*, 2577.

(41) Daura, X.; Gademann, K.; Jaun, B.; Seebach, D.; van Gunsteren, W. F.; Mark, A. E. *Angew. Chem., Int. Ed.* **1999**, *38*, 236.

(42) Mark, A. E. In *Encyclopaedia of Computational Chemistry*; von Rague Schleyer, P., Ed.; John Wiley & Sons Ltd: Chichester, U.K., 1998; Vol. 2, p 1070.

(43) Heelis, P. F. In *Chemistry and Biochemistry of Flavoenzymes*; Müller, F., Ed.; CRC Press: Boca Raton, FL, 1991; Vol. I, pp 171−193.

(44) Tsibris, J. C. M.; McCormick, D. B.; Wright, L. D. *Biochemistry* **1965**, *4*, 504.

(45) Karen, A.; Ikeda, N.; Mataga, N.; Tanaka, F. *Photochem. Photobiol.* **1983**, *37*, 495.

(46) Karen, A.; Sawada, M. T.; Tanaka, F.; Mataga, N. *Photochem. Photobiol.* **1987**, *45*, 49.

(47) Zhong, D.; Zewail, A. H. *Proc. Natl. Acad. Sci. U.S.A.* **2001**, *98*, 11867.

(48) Mataga, N.; Chrosrowjan, H.; Shibata, Y.; Tanaka, F. *J. Phys. Chem. B* **1998**, *102*, 7081.

(49) Mataga, N.; Chrosrowjan, H.; Shibata, Y.; Tanaka, F.; Nishina, Y.; Shiga, K. *J. Phys. Chem. B* **2000**, *104*, 10667.

(50) Rehm, D.; Weller, A. *Isr. J. Chem.* **1970**, *8*, 259 (21st Farkas Memorial Symposium).

(51) Marcus, R. A.; Sutin, N. *Biochim. Biophys. Acta* **1985**, *811*, 265.

(52) Seidel, C. A. M.; Schulz, A.; Sauer, M. H. M. *J. Phys. Chem.* **1996**, *100*, 5541.

(53) Draper, R. D.; Ingraham, L. L. *Arch. Biochem. Biophys.* **1968**, *125*, 802.

(54) Moser, C. C.; Keske, J. M.; Warncke, K.; Farid, R. S.; Dutton, P. L. *Nature (London)* **1992**, *355*, 796.

(55) Stanley, R. J.; MacFarlane, A. W., IV. *J. Phys. Chem. A* **2000**, *104*, 6899.

(56) Park, H. W.; Kim, S. T.; Sancar, A.; Deisenhofer, J. *Science (Washington, D.C.)* **1995**, *268*, 1866.